

## PULSARS

Summer Student Lecture - 29 June 1973

D. C. Backer

### I. DISCOVERY

In 1967 a group of scientists in Cambridge, England undertook a systematic study of the effects of the interplanetary medium on the propagation of radiation, intensity modulation or scintillation, from compact extragalactic sources. For this purpose they constructed a multi-acre array of dipole antennae and began recording the interplanetary scintillations of all sources in the sky. The novel aspect of these observations was that they demanded very little smoothing of the data to detect the rapid (1 Hz) scintillations. Hence, they were the first to survey the sky for sources which were varying rapidly for reasons other than scintillation. A student on the project noted a source of pulsed radiation that recurred day after day. The pulsations were accurately periodic and had a duty cycle of about 3 percent. For three months this object was followed with the utmost of secrecy. After that time they were certain of its cosmic origin for two reasons: it maintained the same position in the celestial sky which meant that it could not be a terrestrial event which recurred daily, and the observed period of the pulsations changed in ways consistent with the variations expected from the Doppler shift of the observatory due to the orbital motion of the Earth about the Sun. Thus their systematic study led to the discovery of a new and unexpected source of radio radiation--pulsating radio stars or pulsars.

Later investigations by the Cambridge group and by scientists at the Mills' Cross in Australia, at Jodrell Bank in England, at the NRAO and at the Arecibo observatory have resulted in a list of 100 pulsars. A current list of objects is given in Table I. The accurate periodicity of the signals from the pulsars is their most distinctive property. The periods are frequently determined to one part in  $10^9$ . This is the accuracy that quartz crystals can be made to oscillate in the laboratory. In astrophysics, this accuracy implies that the phenomenon is in the realm of the mechanics of massive bodies since only these bodies have the inertia to maintain some form of motion with precision. Standard questions about massive objects for the astrophysicist are: (1) what is the characteristic time scale of a body in relation to its mass and radius, and (2) what are the possible equilibrium states, which are required if we expect to see them, of stellar masses? Let me answer the second question first. The garden variety star that you see at night, and the sun, is a mass of hydrogen and other elements which is gravitationally bound and supported against collapse by the pressure of the radiation generated by the grand-scale fusion reaction in its core. It has been known for many years that the dying embers of a star in which fusion reactions have ceased could form a white dwarf with its mass supported against the gravitational collapse by an electron degeneracy pressure, a quantum effect arising

Table I

\*\*\*\*\*GO FT06FO01 \*\*\*\*\*PRINTER2\*\*\*FMT '01' \*\*\*\*\*18 LINES \*\*\* 12:26.36PM 13 MAR 73 CLARK 64 BERGER 64

TERVANT TERZIAN CSRA AND NAIC CORNELL UNIVERSITY \*PULSARS\* MAR. 14, 1973 TOTAL NUMBER= 89 PAGE 1

PULSAR DESIGNATION	PULSAR	R.A. H.M.S.	DECL. DEG. ' "	L I I DEG.	B I I DEG.	PERIOD (SEC)	EPOCH (J.D.24+)	WIDTH (MSEC)	DISPERSION MEASURE (PARSEC/CM3)	PERIOD CHANGE (INSEC/DAY)	APP. AGE P(10P/DT)
P0031-07	MP0031	0 31 36	-07 38 26	110.4	-69.8	0.9429507566	40690	51.0	10.69	0.0366	7.1E+07
P0105+65	PSR0105+65	1 05 00	65 50	124.6	3.3	1.283651	41554	(29)	30		
P0138+59	PSR0138+59	1 38 59	59 45	129.1	-2.3	1.222949	41544	35	34.5		
P0153+61	PSR0153+61	1 53 00	61 55	130.5	0.2	2.351615	41554	(43)	60		
P0254-54	MP0254	2 54 24	-54	270.9	-54.9	0.4476	(41347)	10	10		
P0301+19	PSR0301+19	3 01 45	19 23 36	161.1	-33.2	1.38758356	41347	27	15.7		
P0329+54	CP0329	3 29 11	54 24 38	145.0	-1.2	0.71451864244	40622	6	26.776	0.177	1.1E+07
P0355+56	PSR0355+56	3 55 03	54 13	148.1	0.9	0.15638004	41594	3.5	57.0		
P0459-18	MP0450	4 50 22	-18 04 14	217.1	-34.1	0.548935369	41536	19	39.9		
P0525+21	MP0525	5 25 52	21 58 18	183.8	-6.9	3.7454934468	40957	181.0	50.8	3.461	2.9E+06
P0531+21	MP0531	5 31 31	21 58 55	184.6	-5.8	0.0331296454	41221	3	56.805	36.526	2.5E+03
P0540+23	PSR0540+23	5 40 10	23 30	184.4	-3.3	0.245964	41554	(16)	72		
P0511+22	PSR0511+22	6 11 03	22 35	188.7	2.4	0.33491850	41603	(8)	96.7	7.377	1.3E+05
P0528-28	PSR0628-28	6 28 51	-28 34 08	237.0	-16.8	1.244414895981	40242	(50)	34.36	0.217	1.6E+07
P0736-47	MP0736	7 36 51	-40 35 18	254.2	-9.2	0.374918324	40221	22	100	<1.728	>5.9E+05
P0740-28	PSR0740-28	7 40 48	-28 15 16	243.8	-2.4	0.166750167	41027	8	80		1.9E+05
P0809+74	CP0809	8 09 03	74 38 10	140.0	31.6	1.2922412452	40689	41.3	5.84	0.0138	2.5E+08
P0819-13	MP0819	8 18 06	-13 41 23	235.9	12.6	1.23612810726	41006	22	40.9	0.1820	1.9E+07
P0823+26	AP0823+26	8 23 51	26 47 18	197.0	31.7	0.53065959042	40242	5.9	19.4	0.144	1.0E+07
P0833-45	PSR0833-45	8 33 39	-45 00 11	263.6	-2.8	0.082187479	40307	63	10.823		2.3E+04
P0834+06	CP0834	8 34 26	06 20 47	219.7	26.3	1.27376349759	40626	23.7	12.90	0.587	5.9E+06
P0835-41	MP0835	8 35 34	-41 24 54	260.9	-0.3	0.76698	(41347)	20	120		
P0904+77	PSR0904+77	9 04 07	77 40	135.3	33.7	1.57905	(40222)	<80			
P0940-56	MP0940	9 40 40	-56	278.8	-2.5	0.662	(40402)	30	145		
P0943+10	PP0943	9 43 20	10 05 33	225.4	43.2	1.097707	40519	50	15.35		
P0950+08	CP0950	9 50 31	08 09 43	228.9	43.7	0.25306504317	40622	8.8	2.965	0.0198	3.5E+07
P0959-54	MP0959	9 59 51	-54 37	280.1	0.3	1.436551	40553	50	90		
P1055-51	MP1055-51	10 55 49	-51 40	286.0	7.0	0.1971	(41347)		<30		
P1112+50	PSR1112+50	11 12 49	50 40	155.1	60.7	1.65643810	41594	14	9.2		
P1133+16	CP1133	11 33 28	16 07 33	241.9	69.2	1.18791116405	40622	27.7	4.834	0.323	1.3E+07
P1154-62	MP1154	11 54 45	-62 08 36	296.7	-0.2	0.40052	(41347)		270		
P1237+25	AP1237+25	12 37 12	25 10 17	252.2	86.5	1.38244857195	40626	49.9	9.254	0.0825	4.6E+07
P1249-46	MP1240	12 40 20	-46 07 12	302.1	-1.6	0.38850	(41347)	60	220		
P1321-62	PSR1321-62	13 23 42	-62 03	307.1	0.3	0.529854	41733		313		
P1354-62	PSR1354-62	13 54 10	-62 13	310.5	-0.6	0.455780	41733		400		
P1359-50	MP1359	13 59 43	-50	314.5	11.0	0.690	(40585)	20	20		
P1426-66	MP1426	14 26 34	-66 09 54	312.3	-6.3	0.7874	(41347)	10	60		
P1447-55	MP1449	14 49 22	-55	315.3	-5.3	0.180	(40282)	(5)	90		
P1451-68	PSR1451-68	14 51 29	-68 32	313.9	-8.6	0.263376764	(40545)	25	8.6	<0.259	>2.8E+06
P1508+55	MP1508	15 08 04	55 42 56	91.3	52.3	0.73967787630	40626	10.3	19.60	0.433	4.7E+06
P1530-53	MP1530	15 30 23	-53 30	325.7	1.9	1.368892	40553	25	20		
P1541+09	AP1541+09	15 41 14	09 38 43	17.8	45.8	0.7484483	(41347)	63	35.0		
P1556-44	MP1556	15 56 12	-44 31 30	334.5	6.4	0.25705	(41347)				
P1558-50	PSR1558-50	15 58 46	-50 49	330.7	1.3	0.864192	41733		165		
P1601-52	PSR1601-52	16 01 58	-52 56	329.7	-0.6	0.657953	41733		35		
P1604-00	MP1604	16 04 38	-00 24 41	10.7	35.5	0.42181607579	41005	15	10.72	0.0265	4.4E+07
P1641-45	PSR1641-45	16 41 09	-45 51	339.2	-0.2	0.454963	41733		449		
P1642-03	PSR1642-03	16 42 25	-03 12 30	14.1	26.1	0.38768877965	40622	3.7	35.71	0.154	6.9E+06
P1700-18	MP1700-18	17 00 56	-18	4.0	14.0	0.802	(41347)		<40		
P1706-16	MP1706	17 06 33	-16 37 21	5.8	13.7	0.65305045437	40622	12	24.99	0.550	3.3E+06
P1717-29	PSR1717-29	17 17 10	-29 32	356.5	4.3	0.620449	41554	(32)	45		
P1718-32	PSR1718-32	17 18 40	-32 05	354.5	2.5	0.477154	41554	(35)	120		
P1727-47	MP1727	17 27 59	-47 42 18	352.6	-7.6	0.829683	40553	30	121		
P1747-46	MP1747	17 47 56	-46 56 12	345.0	-10.2	0.742349	40553	20	40		
P1749-29	PSR1749-29	17 49 49	-29 06 00	1.5	-1.0	0.562553168299	40127	6	50.88	0.705	2.2E+06
P1818-04	MP1818	18 18 14	-04 29 03	25.5	4.7	0.59807262183	40622	10.3	84.48	0.545	3.0E+06
P1819-22	PSR1819-22	18 19 50	-22 53	9.4	-3.3	1.874398	41554	(76)	14.3		
P1822-09	PSR1822-09	18 22 40	-09 36	21.4	1.3	0.768948	41554	11	20.3		
P1826-17	PSR1826-17	18 26 15	-17 54	14.6	-3.3	0.307128	41554	(59)	10.7		
P1831-03	PSR1831-03	18 31 02	-03 40	27.7	2.3	0.686675	41554	(32)	235		
P1845-01	OP1845-01	18 45 01	-01 27	31.3	0.2	0.659475	(41192)	(80)	90		
P1845-04	JP1845	18 45 10	-04 05 32	28.9	-1.0	0.59773452	40988	20	141.9		
P1846-06	PSR1846-06	18 46 07	-06 43	26.7	-2.4	1.451323	41554	(38)	152		
P1857-26	MP1857	18 57 44	-26 04 49	10.5	-13.5	0.612204	41026	25	35		
P1858+33	JP1858	18 58 40	03 27 02	37.2	-0.6	0.655444	40754	(170)	402		
P1900-06	PSR1900-06	19 00 30	-06 35	28.5	-5.6	0.431885	41554	(14)	180		
P1907+02	PSR1907+02	19 07 20	02 56	37.7	-2.7	0.494914	41554	(11)	190		
P1911-04	MP1911	19 11 15	-04 45 59	31.3	-7.1	0.82593366503	(40624)	8.0	89.41	0.351	6.5E+06
P1915+13	OP1915+13	19 15 25	13 50 00	48.3	0.6	0.1946255	41274	15	94		
P1917+00	PSR1917+00	19 17 15	00 18	36.5	-6.1	1.272254	41554	(27)	85		
P1919+21	CP1919	19 19 36	21 47 17	55.8	3.5	1.33730115212	40690	31.2	12.43	0.116	3.2E+07
P1929+10	PSR1929+10	19 29 52	10 53 03	47.4	-3.9	0.22651703833	40625	5.3	3.176	0.100	6.2E+06
P1933+16	JP1933+16	19 33 32	16 09 58	52.4	-2.1	0.3587352051	40690	8.0	158.53	0.519	1.9E+06
P1944+17	MP1944	19 44 39	17 58 44	55.3	-3.5	0.4406179	(40618)	30	16.3		
P1946+35	JP1946	19 46 35	35 28 36	70.6	5.0	0.717306	40659	21	129.1		
P1953+27	JP1953	19 53 00	27 15 03	66.0	0.7	0.426676	40754	13	20		
P2002+30	JP2002	20 02 35	30	67.7	-0.7	2.111206	40756	15	233		
P2016+28	PSR2016+28	20 16 02	28 30 31	68.1	-4.0	0.55795339053	40689	13.9	14.16	0.0129	1.2E+08
P2020+28	PSR2020+28	20 20 33	28 44 30	68.9	-4.7	0.34300790	41348	6.7	24.6		
P2271+51	JP2021	20 21 25	51 45 08	87.9	8.4	0.52919531221	40626	6.6	22.580	0.263	5.5E+06
P2045-16	PSR2045-16	20 45 47	-16 27 48	30.5	-33.1	1.98156682076	40695	79.0	11.51	0.945	5.7E+06
P2111+46	MP2111	21 11 39	46 31 42	89.0	-1.3	1.01468444509	41006	29	141.4	0.0620	4.5E+06
P2148+63	PSR2148+63	21 48 03	63 10 42	104.1	7.4	0.38082	41554	(29)	125		
P2156+40	PSR2156+40	21 56 54	40 02 30	90.5	-1.4	1.252534	41532	52	71.0		
P2217+47	PSR2217+47	22 17 46	47 39 48	98.4	-1.6	0.53846737844	40624	7.9	43.52	0.239	6.2E+06
P2256+58	PSR2256+58	22 56 30	58 50	108.8	-0.7	0.368241	41554	(14)	148		
P2303+30	AP2303+30	23 03 14	30 43 49	97.7	-26.7	1.575884410	41006	26.0	49.9	0.2514	1.7E+07
P2305+55	PSR2305+55	23 05 00	55 26	108.6	-4.2	0.475068	41554	(27)	45		
P2319+60	JP2319	23 19 42	60 00	112.0	-0.6	2.25648387	41536	65	96		

from the fact that electrons are fermions. These objects have been detected amongst the local stars. In 1939 theoretical models of the neutron star predicted by Landau in 1932 were developed by Oppenheimer and Volkoff as a byproduct of atomic bomb research; its mass would be supported against collapse by a nuclear degeneracy pressure. Baade and Zwicky had suggested in 1934 that these objects might be formed in supernova explosions. Recently much interest has been devoted to an additional object where the collapse could not be averted; the mass disappears into a black hole, so called since light cannot escape from the surface of the object. A back-of-the-envelope calculation of the vibrational time scale for any object is found by setting the gravitational acceleration at the surface,  $GM/R^2$ , equal to an acceleration of a point mass dropped into the center,  $R/t^2$ . This results in  $t \sim (G\rho)^{-1/2}$  where  $\rho$  is the density  $M/R^3$ . A similar calculation for a rotational time scale comes from setting the surface gravitational acceleration equal to the centrifugal force. This results in the same estimate for  $t$ . For the tremendous density of  $10^{14}$  gm/cm<sup>2</sup>, the density at which neutrons become degenerate,  $t \sim 1$  ms. Incidentally, a solar mass at these densities occupies a ball about 10 km in radius and acts very much like an atomic nucleus with an atomic number of  $10^{57}$ .

Another speculation about these star embers in prepulsar days was that the magnetic fields could be large as a result of the collapse or implosion of a large star. Consider the Sun with a one Gauss field ( $B_{\odot}$ ). Now allow the Sun to contract from  $R_{\odot}$  to a radius  $R$  while conserving magnetic flux:  $\phi \sim B_{\odot} R_{\odot}^2 \sim BR^2$ . The new field  $B \sim B_{\odot} R_{\odot}^2/R^2$ . This results in predictions of  $10^6$  Gauss for white dwarfs ( $R \sim 10^8$  cm), which has been measured in one case, and  $10^{11}$  Gauss for neutron stars ( $R \sim 10^6$  cm).

Considering the matrix of attractive possibilities to explain pulsars, white dwarf/neutron star and rotation/vibration, Professor Gold was convinced that the objects were rotating, magnetic neutron stars. In his model the magnetic field is forced into corotation by magnetohydrodynamic forces arising from its plasma content. However this "magnetosphere" of the neutron star would run into trouble at a distance from the axis of rotation  $R_C$  where the corotation at constant angular frequency  $\Omega$  forces the field and plasma to the speed of light,  $R_C = c/\Omega$ . Gold felt that there would be some interaction on this "light cylinder" causing the corotation to stop and producing anisotropic radio radiation which we view as pulses just as one views a revolving beacon from a lighthouse. The great prediction of this model was that the pulsar periods would decay with time due to a loss of rotational energy. This was contrasted with vibrational models where energy loss leads to collapse, to higher densities, and hence to shorter period oscillations. Furthermore, Gold predicted that, since the time scale  $t$  for neutron stars could extend down to 1 ms, young, short period pulsars remained to be detected. Both the period increase with time and a young short period pulsar were detected.

## II. PROPAGATION PHENOMENA

The pulsar emission arrives in short pulses when observed with a narrow bandwidth at any radio frequency. A comparison of the outputs from two such bandwidths with center frequencies offset by a few MHz shows that the pulses arrive at a later time at lower frequencies. When extension is made to larger frequency offsets, it is found that the delay between pulses has a quadratic dependence on frequency. Because the pulse arrival time is frequency dependent we say the pulsar radiation is dispersed. The microscopic interaction between electromagnetic waves and matter in the transmitting medium causes a wave packet to travel at speeds less than  $c$ ; that is, the group velocity is less than  $c$ . If the interaction is frequency dependent, the medium is called dispersive. A plasma is a dispersive medium and from Maxwell's equations one can find a dispersion relation between the index of refraction and the radio frequency. From this the group velocity is derived. For a tenuous plasma with only the interaction with the electrons considered and with negligible magnetic field this velocity is

$$v_g/c = 1 - n_e e^2 / (2\pi m_e c^2 \nu^2), \text{ if } \nu_p = \sqrt{\frac{n_e e^2}{2\pi m_e c^2}} = \text{plasma frequency.} \\ \text{is } \ll \nu.$$

The dispersion delay between frequencies  $\nu_1$  and  $\nu_2$  is

$$\tau_d = (1/\nu_2^2 - 1/\nu_1^2) \frac{e^2}{2\pi m_e c} \int n_e d\ell = (1/\nu_2^2 - 1/\nu_1^2) (\int n_e d\ell / 2.41 \times 10^{-4}).$$

This relation accurately describes all observations of pulse arrival delay with frequency. The dynamic spectrum of a pulsar is sketched in figure 1. The parameter  $\int n_e d\ell$  has been defined as the dispersion measure (DM) with units of parsecs  $\text{cm}^{-3}$ . The observed range is

$$3 < \text{DM observed} < 400 \text{ pc cm}^{-3}.$$

Where is this plasma? The following table will allow some statements to be made on various hypotheses.

Medium	Electron Density	Depth	D. M. Contribution	Hypothesis Test
Earth Ionosphere	$3 \times 10^5 \text{ cm}^{-3}$	$1.5 \times 10^8 = 5 \times 10^{-11} \text{ pc}$	$2 \times 10^{-5} \text{ pc cm}^{-3}$	No
Interplanetary Medium (away from Sun)	1-10	1 AU = $5 \times 10^{-6}$	$5 \times 10^{-5}$ or 6	No
Interstellar Medium	$\leq 0.1$	300 pc	30	Yes
HII Regions	~1	~10	10	Possible
Pulsar Neighborhood	Crab: 40 Others?	0.5	20	Yes No?

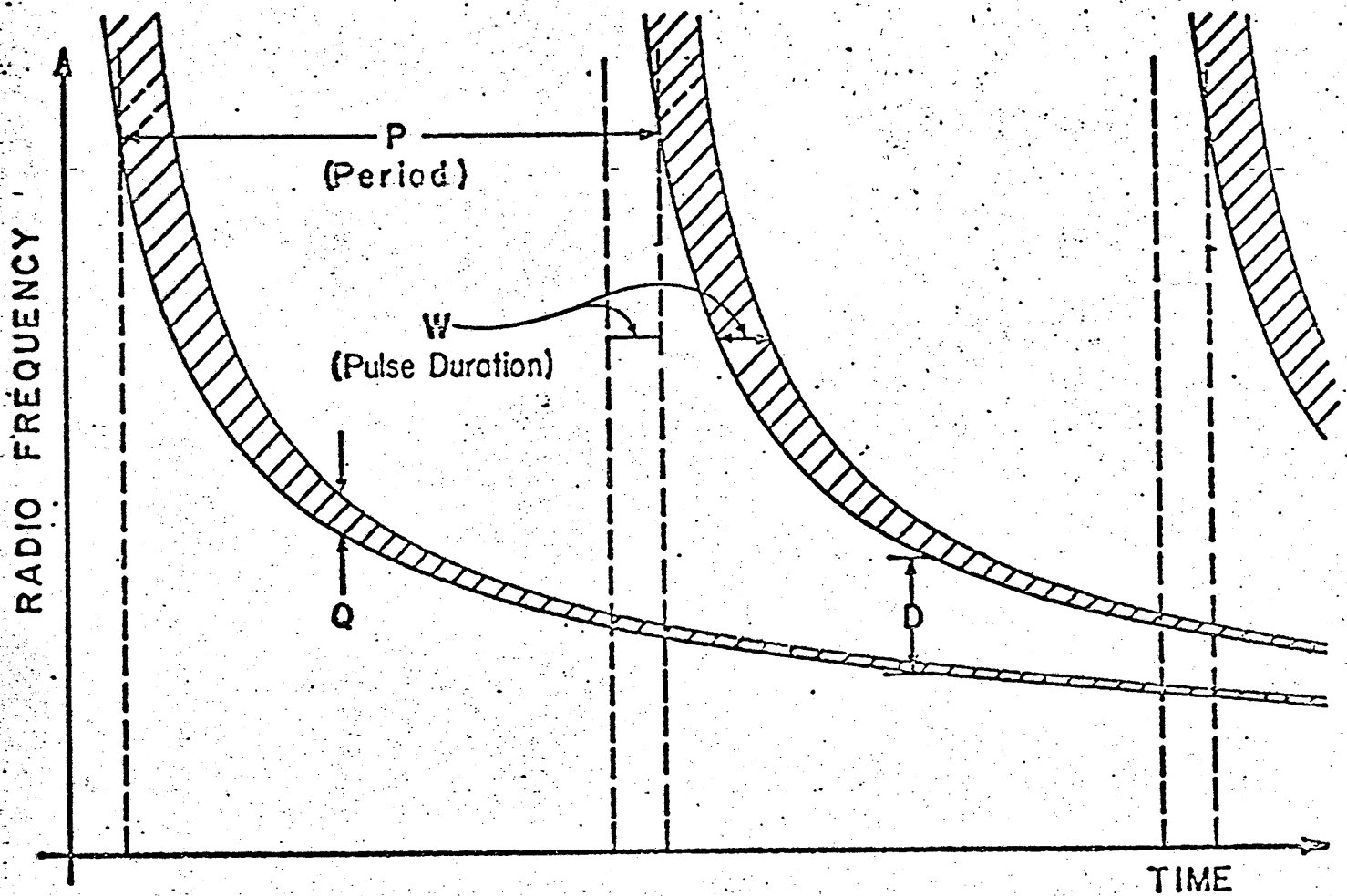


FIG. 1. Pulsar dynamic spectrum. The hatched area indicates region of the frequency-time plane that is occupied by a series of pulses.

Further confidence in attributing the dispersion to the interstellar medium in the general case can be gained from the presentation in figure 2, a correlation diagram of the DM and the galactic latitude  $b^{\text{II}}$ . The correlation is that expected if the pulsars reside near the plane of the galaxy and if the DM comes from plasma distributed in the plane. From the above discussion it is clear that, after corrections are made for obvious HII regions or pulsar associated nebulae, a reasonable distance estimate can be obtained by dividing the DM by the average electron density  $\langle n_e \rangle$ . It is certain the medium is not uniform, but on a statistical basis these estimates should be valid.

The nonuniformity of the medium plays an important role in the observations of pulsars. There is a simple approach to this which will serve to illustrate the relation between various parameters. The rays from a pulsar are bent by the plasma irregularities which act as giant lenses, a macroscopic description of the microscopic scatterings described above. The rays observed are spread over an angle  $\theta_s$ . Due to geometrical path length differences for rays arriving from angles extending to  $\theta_s$ , a pulse will be spread over a time  $\tau_b$ . The mixture of signals with different delays gives rise to interference of the signal across the radio spectrum with a scale of  $B_s \sim 1/2\pi \tau_b$  and a depth of modulation  $m$ . Finally if there is a velocity of the entire scattering medium relative to the pulsar-observer line of sight, from Earth, pulsar or medium motion, then the interference which also varies spatially at a fixed frequency will give rise to slow temporal variations with a time scale  $\tau_s = a_p/v$ ;  $a_p$  is the interference pattern scale size and  $v$  is the relative velocity. Given this model of the phenomenon, two telescopes spaced by a large fraction of  $a_p$  will measure an offset in time of arrival of the same temporal variations  $\Delta t = d/v$ , where  $d$  is the projected separation of the telescopes.

Figure 3 is a sketch of the dynamic spectrum, with the axes compressed over that of figure 1, which includes paths of individual dispersed pulses and "islands" of constructive interference in the frequency-time plane. In figure 4 the variations of the scale sizes of the islands,  $B_s$  and  $\tau_s$ , and of the depth of modulation,  $m$ , with radio frequency are shown. Below 1-10 GHz the medium severely modulates the radiation. The modulation measure  $m$  is unity, the bandwidth  $B_s$  varies as  $\nu^4$  and the time scale  $\tau_s$  varies as  $\nu$ . Above 1-10 GHz  $m$  decreases as  $\nu^{-1}$ ,  $B_s$  increases less rapidly and  $\tau_s$  is roughly constant. Figure 5 displays observational results from  $B_s$  and  $\tau_b$  as a function of  $\nu$  and DM. The quadratic dependence of  $B_s$  and  $\tau_b^{-1}$  on DM is proof that the scintillation arises in the general interstellar medium.

All of these phenomena are areas of current experimental and theoretical investigations. The simple theory indicates that the scale of the fluctuations is very small,  $\sim 10^{11}$  cm, which is difficult to reconcile with the knowledge of lifetimes of density irregularities of that scale.

Observations of the local magnetic field in the interstellar medium are possible by measuring the Faraday rotation of the plane of polarization of the linearly polarized component of pulsar radiation. The rotation occurs because orthogonal propagation modes in a tenuous magnetoionic medium are circularly polarized and travel with different phase velocities. Linearly



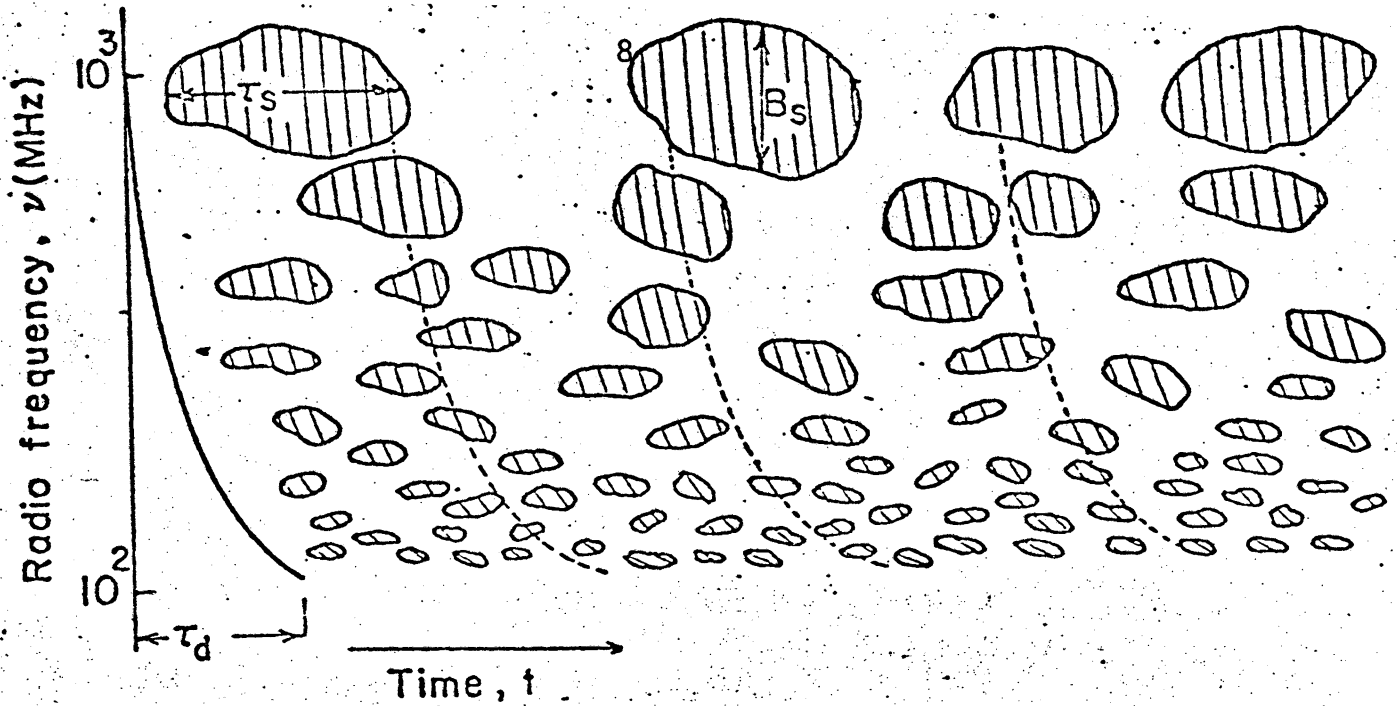


FIG. 3. Pulsar dynamic spectrum. The pulsar signal is only observed within "interference islands" caused by propagation in the interstellar medium.

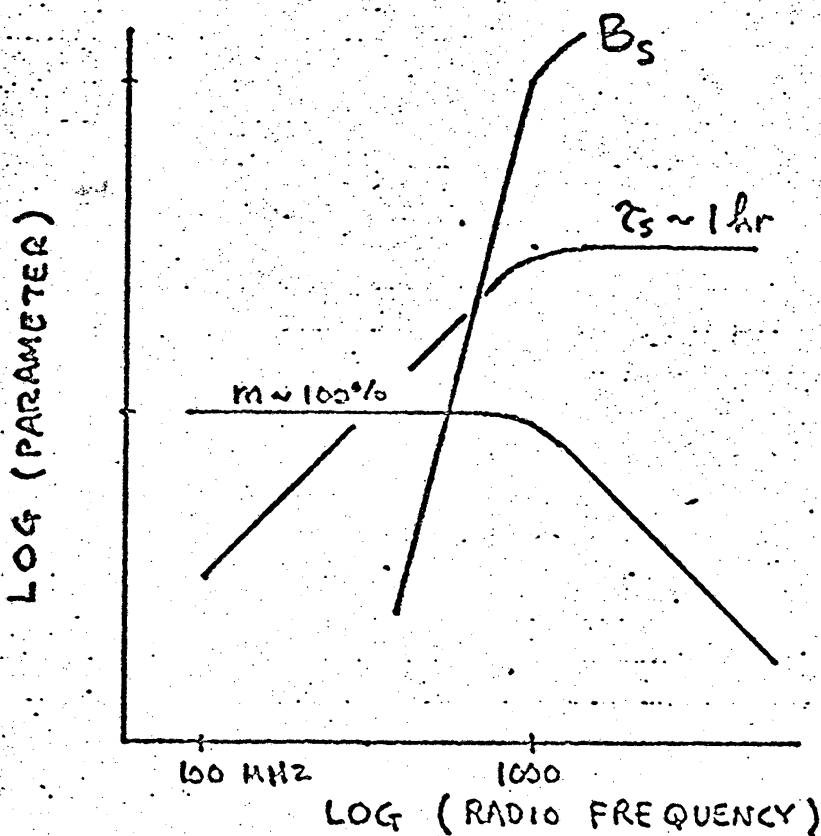


FIG. 4. Variation of the scale of the "interference islands"  $B_s$  and  $\tau_s$  and the depth of modulation  $m$  with frequency-typical pulsar.

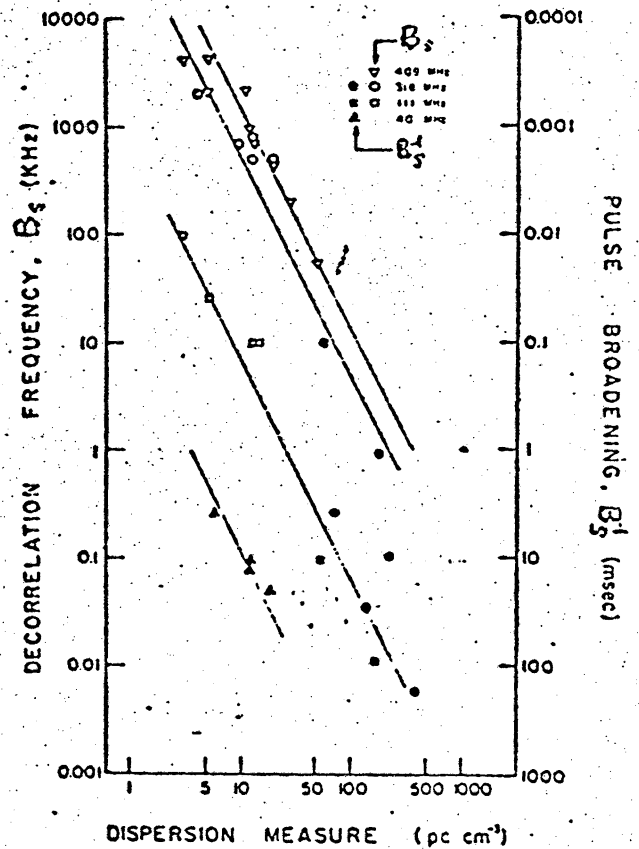


FIG. 5. Observed scintillation parameters as a function of  $\nu$  and DM.

polarized radiation can be viewed as the sum of oppositely-winding, circularly-polarized electric fields. Because the phase velocities of the two circular components of linearly polarized radiation are different, the observed angle of the radiation is rotated from its emitted position. The rotation varies with wavelength  $\lambda$  as

$$\Delta \phi = \int B_{||} n_e d\lambda (\lambda_2^2 - \lambda_1^2) \text{ radians,}$$

where  $B_{||}$  is the component of the magnetic field along the line of sight to the pulsar;  $\int B_{||} n_e d\lambda$  is called the rotation measure (RM). The average field is

$$\langle B_{||} \rangle = \int B_{||} n_e d\lambda / \int n_e d\lambda \approx \text{RM/DM} .$$

### III. INTRINSIC PHENOMENA

Many studies have been made of phenomena intrinsic to the radiation mechanism of the pulsars. One fundamental property of a radio source is the spectrum of its emission. In pulsars measurements are made simultaneously over all frequencies and for long enough to remove the effects of interstellar scintillation. Several examples are shown in figure 6 which give the flux density averaged over the pulse period against radio frequency. These three examples show the full range of pulsar spectra: single power law, high-frequency power law with a flattening at low frequencies, and high-frequency power law with a turnover at low frequencies. What particle configuration are we viewing that radiates with such spectra? A standard argument in astrophysics is that if the power from an object varies over a time  $t$ , then the size of the emitting region must be less than the light-travel distance  $ct$ , so that the emitting particles can pass information to each other about variations. In the pulsars  $t$  is, for example, 100  $\mu\text{sec}$ . For a 1000 flux unit ( $10^{-26} \text{ W m}^{-2} \text{ Hz}^{-1}$ ) emission level at a wavelength of one meter from a source at 300 pc, this implies a brightness temperature from the Planck law of  $10^{28}$  Kelvins (K). Such a temperature cannot be from particles radiating incoherently since their energy would need to be  $10^{24}$  eV. Such energetic charges, if they could be generated, would radiate extremely high frequency photons, not radio waves. (The most energetic cosmic ray particles are  $\sim 10^{20}$  eV.) To explain the  $10^{28}$  K it is necessary to invoke a coherent radiation mechanism, one in which the radiation of one charge is electrically in phase with the radiation of others, where  $N$  particles act in unison and behave as a single ion with charge  $N$ . Such coherent effects allow an enhancement of brightness temperature over incoherent mechanisms by a factor of  $N$ . To reduce  $10^{28}$  K to plausible values for relativistic particles roughly  $10^{20}$  particles are needed in a volume less than  $(ct)^3 \sim 3 \times 10^7 \text{ cm}^3$ . It is perhaps instructive to note that the one coherent source outside our solar system which was in the books before pulsars were discovered turned out to be a pulsar, the compact object in the Crab Nebula. (Furthermore it had been suggested in 1967--

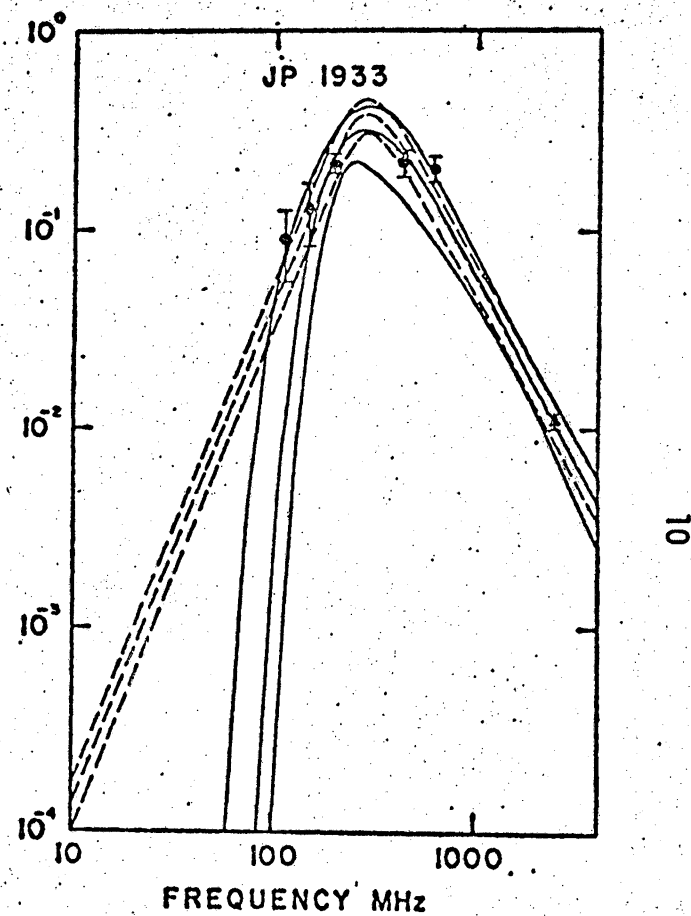
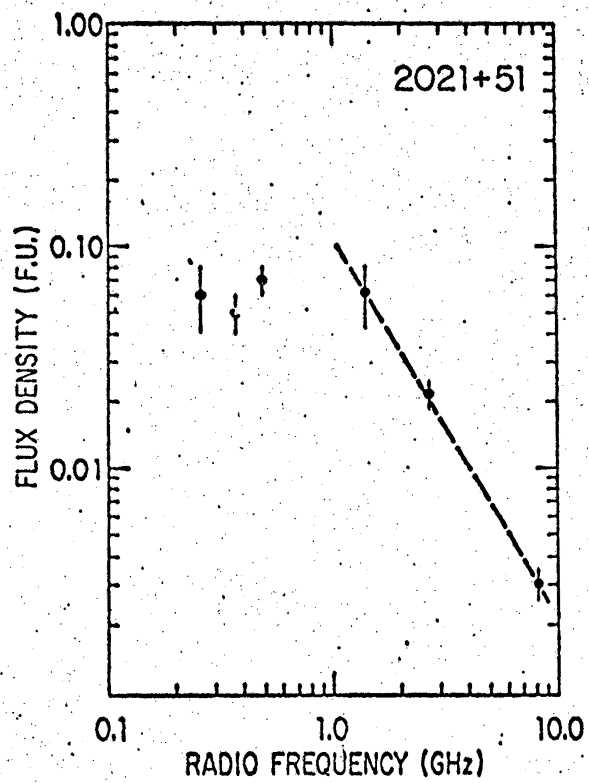
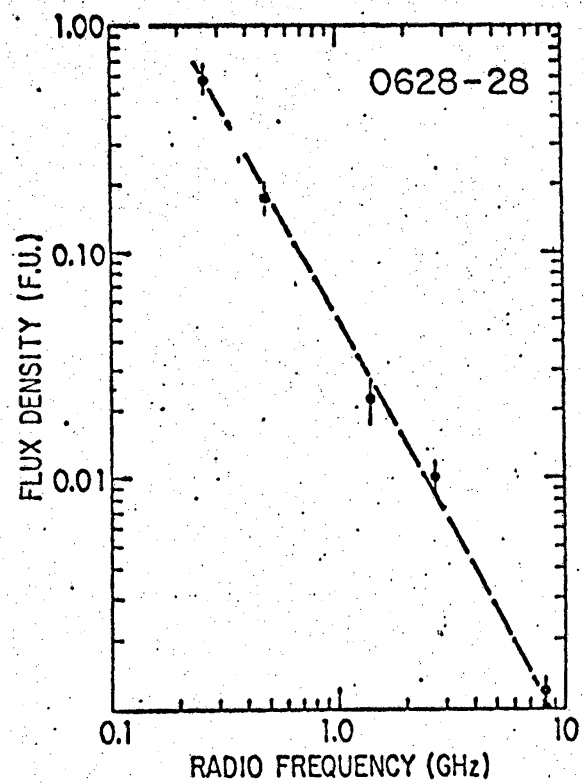


FIG. 6. Pulsar radio spectra. For pulsars 0628-28 and 2021+51 a rough power-law fit has been made to the high frequency data. For JP1933 fits to a power-law with two low-frequency turnovers has been made.

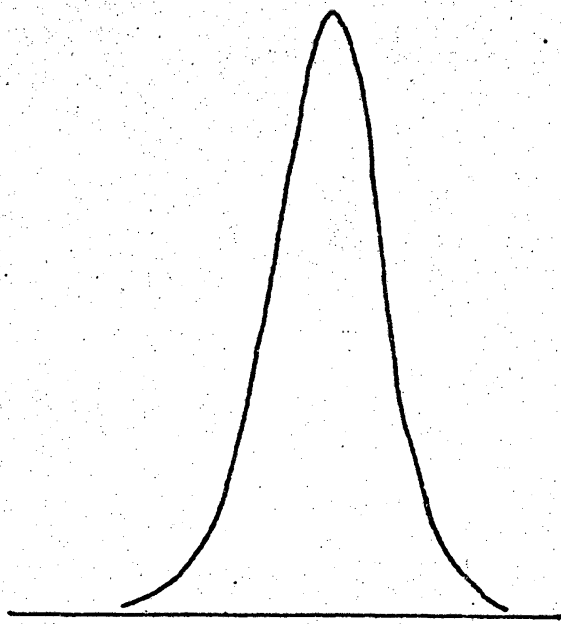
prepulsars--by Pacini that there was a spinning, magnetized neutron star in the Crab Nebula; unfortunately he did not consider that it might be equipped with a "bell".)

The existence of power-law spectra suggests an independence of the radiators at widely separated frequencies--in thermal sources the shape of the long-wavelength, "Planck-law" portion of the spectrum arises from the variation of the number of independent encounters of ions in the sources at a given separation and in nonthermal, synchrotron sources power-law spectra result from the number distribution of independent particles with a given energy. It is likely then that in a pulsar the number of particles with a given parameter varies as the parameter varies and that the parameter has a one-to-one relation to the radio frequency emitted. At present we do not know what this parameter is. In objects where there is a break in the spectrum it is obvious that some fundamental scale is reached, possibly a length scale related to the break frequency by  $c$ .

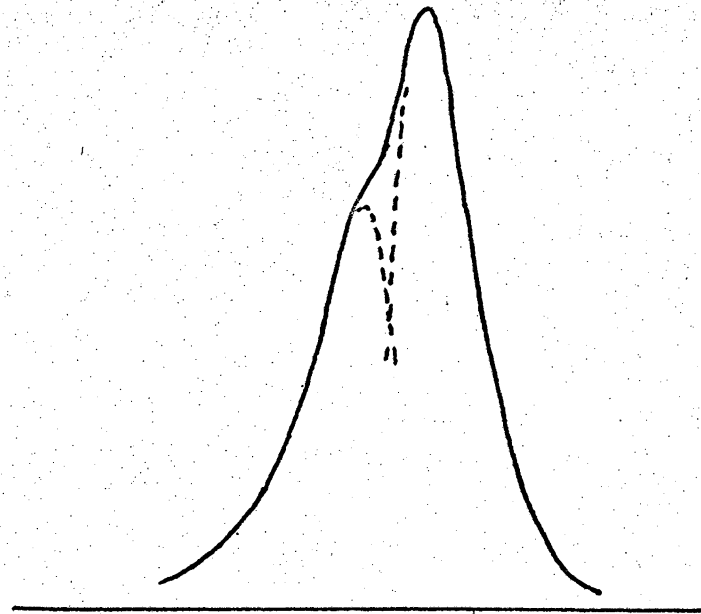
An average of the radiation synchronously with the pulse period produces a pulse profile which is characteristic for each object. These often show the presence of components, or distinct regions within the pulse emission window. A recent investigation shows that all profiles can be broken down into two fundamental profiles--one with a single-peak and one with a double peak. The fundamental components are sketched in figure 7 along with the decompositions of several pulse profiles. Not included in the above description are various forms of radiation which extend beyond the narrow 3 percent of the period. Several of the shortest period pulsars, 0531+21 (.033 s), 1929+10 (.226), 0950+08 (.253), 0823+26 (.531), and possibly two others, have emission nearly midway between pulses and in fact 0531+21, 0950+08, and 1541+09 have pulsed emission over 50% of their period (figure 8). These profiles have a constant morphology in time over intervals of a year but do change in the relative amplitudes of their components. The separation of double fundamental profiles decreases slowly with increasing frequency ( $\sim \nu^{-1/4}$ ) in many objects.

Our knowledge of the guts of a pulsar is in a primitive state. The components of a pulse referred to above may represent separate streams of charges from the central star which radiate in our direction once per pulse period as a consequence of the rotation. Another view is that the components represent a variation of the efficiency of the production of coherent radiation with angle across a wide stream of charges.

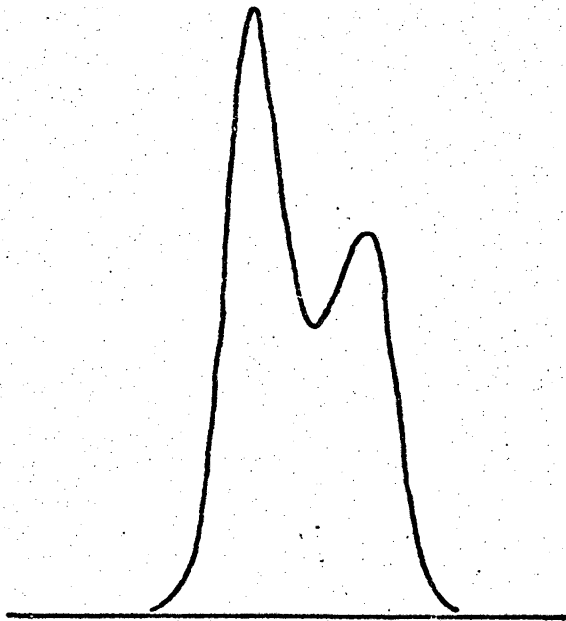
The extremely strong magnetic fields predicted are required in most models of the emission mechanisms to provide a means of accelerating the charges--the rotating field acts as a unipolar inductor and can generate potential drops of  $10^{13}$ - $10^{15}$  volts which develop currents  $\sim 10^{11}$ - $10^{13}$  amperes flowing through an area whose dimensions may be about the size of University Hall. The energy output is then  $10^{31}$ - $10^{35}$  ergs/sec which is large compared to terrestrial standards--radar, lightning, laboratory plasma beams--and to solar system standards--solar bursts and Jupiter bursts, but insignificant next to the energetics of compact extragalactic objects. A large current



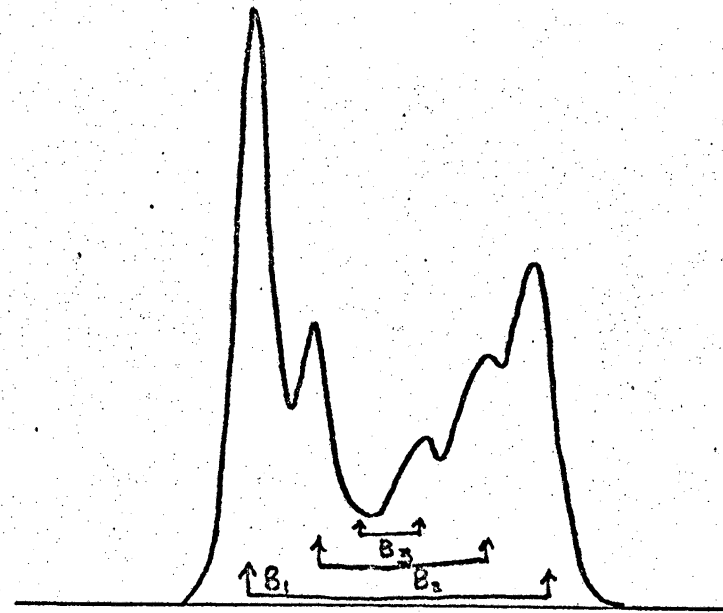
A-SINGLE (0823+26)



0950+08 - B (HIDDEN)



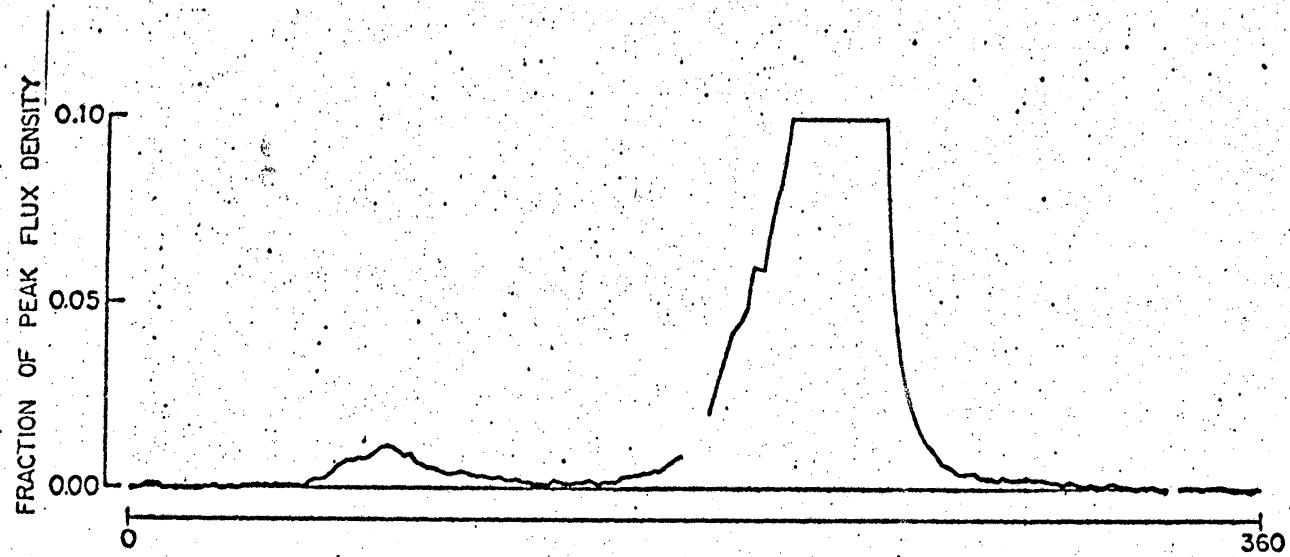
B- DOUBLE (0834+06)



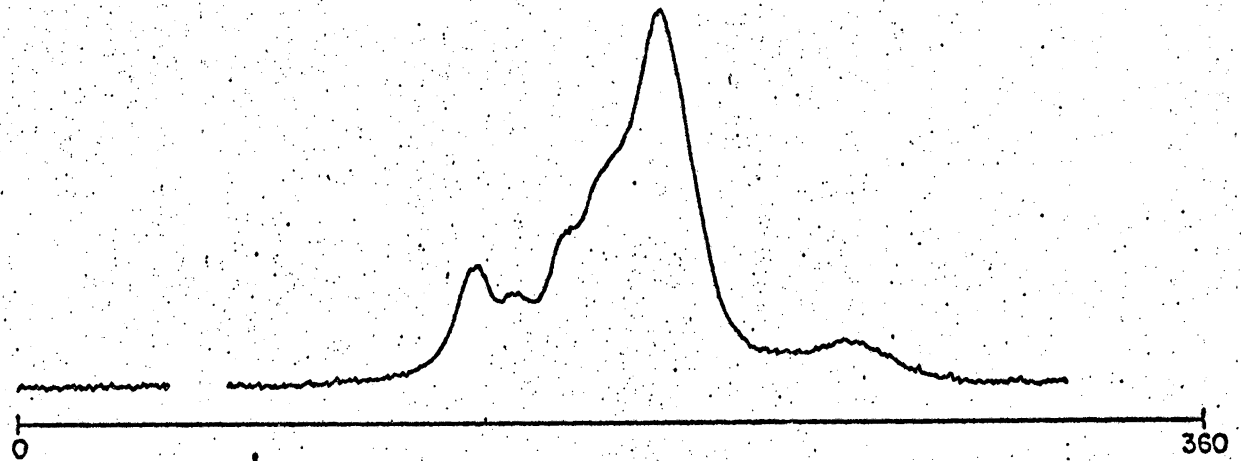
1237+25 -  $B_1 + B_2 + B_3$

FIG. 7. Fundamental pulse profile components. To the left are two fundamental pulse components observed--single and double. To the right are the suggested decompositions of two pulsars into fundamental components.

0950+08  
430 MHz



1541+09  
430 MHz



0531 + 21  
318 MHz

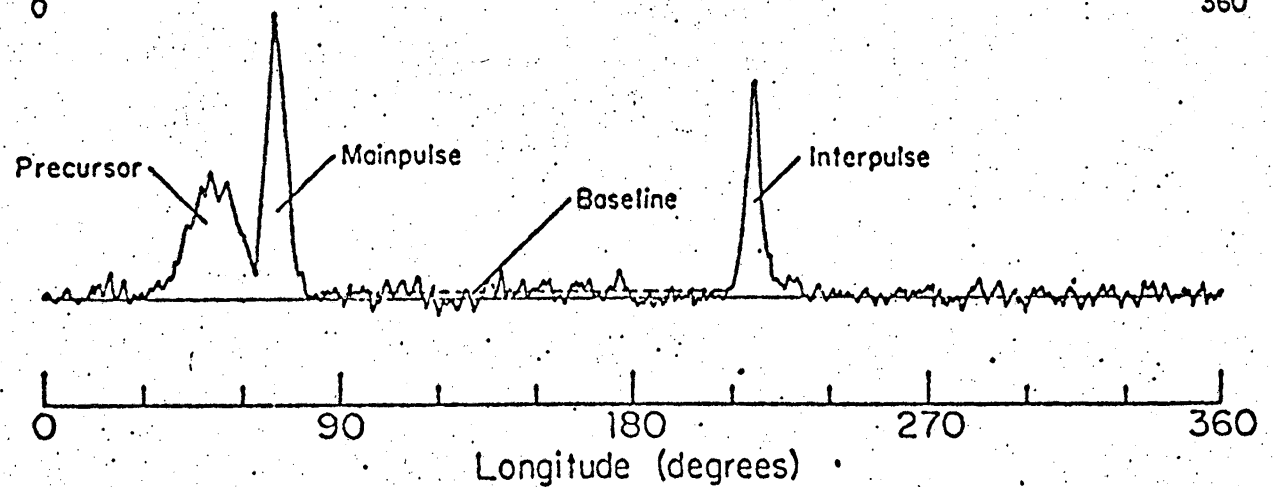


FIG. 8. Full-period profiles of three pulsars showing extended emission.

flowing along curved magnetic field lines may be the source of the observed radiation; such an emission mechanism would produce the high degrees of polarization which we observe--in cases nearly 100%. The angle of the linearly polarized radiation often varies smoothly across the fundamental components of a pulse but may show complex behavior when a profile consists of more than one fundamental component. Compare in figure 9 PSR 0628-28 and PSR 0823+26 with PSR 2020+28 which consists of two "single" fundamental components. The polarization angle variation has been shown to be similar over a wide range of frequencies which suggests that it may be related to a geometrical effect such as the orientation of the pulsar spin axis and magnetic pole relative to the line of sight. In PSR 0823+26 there is an intriguing sign change of the circular polarization across its single component. Polarization phenomena then are an important tool for investigating the pulsar emission mechanism.

The pulsar emission varies on every time scale that has been investigated. These are summarized in autocorrelation functions and data displays in figure 10. The minute-to-hour variations arising from propagation effects have already been discussed (figs. 3-4 and fig. 10c). The finest scale variations in pulsars, at the moment, are micropulses which last for 10-100  $\mu$ sec, or 0<sup>o</sup>015-0<sup>o</sup>03 when measured in longitude (fig. 10a). These probably arise from "coherence noise" in the emission mechanism. Moderate time resolution investigations of single pulses showed that individual pulses seldom mimic the average profile; usually individual pulses consist of one or more subpulses with a scale of  $\sim 1^\circ$  of longitude (fig. 10b). These may arise from a particle stream or a particle bunch or from a favored direction for amplification of radiation to the coherent brightness temperature. In many objects the subpulses are correlated in a short sequence of pulses indicating that the pulsar "remembers" the physical structure which led to their production. In other cases or in parallel there is randomness to the position and amplitude of the subpulses --the resulting average profile is then a statistical mean of the individual pulse behavior.

Beyond the variations lasting a few pulse periods (2 to  $\sim 10$  periods), there is a domain between 50 and 200 periods where correlated variations are observed (fig. 10c). Finally recent studies have shown that the average flux of some pulsars varies on weekly time scales (fig. 10d). All these forms of memory in the pulsar are telling us something important --but at the moment we do not know what in detail.

#### IV. SOME CORRELATIONS

Pulse periods are lengthening slowly with time. The spin-down rate  $\dot{P}$  can be used to compute a spin-down time  $\tau = P/\dot{P}$ . In figure 11 it is shown that a correlation exists between spin-down age and period. This fits the concept that all pulsars are born with short periods and evolve over a million years to long periods as they lose energy. Other interpretations are, of course, possible. In figure 12 it is shown that there is a period-luminosity relationship, which may be an evolutionary effect also.

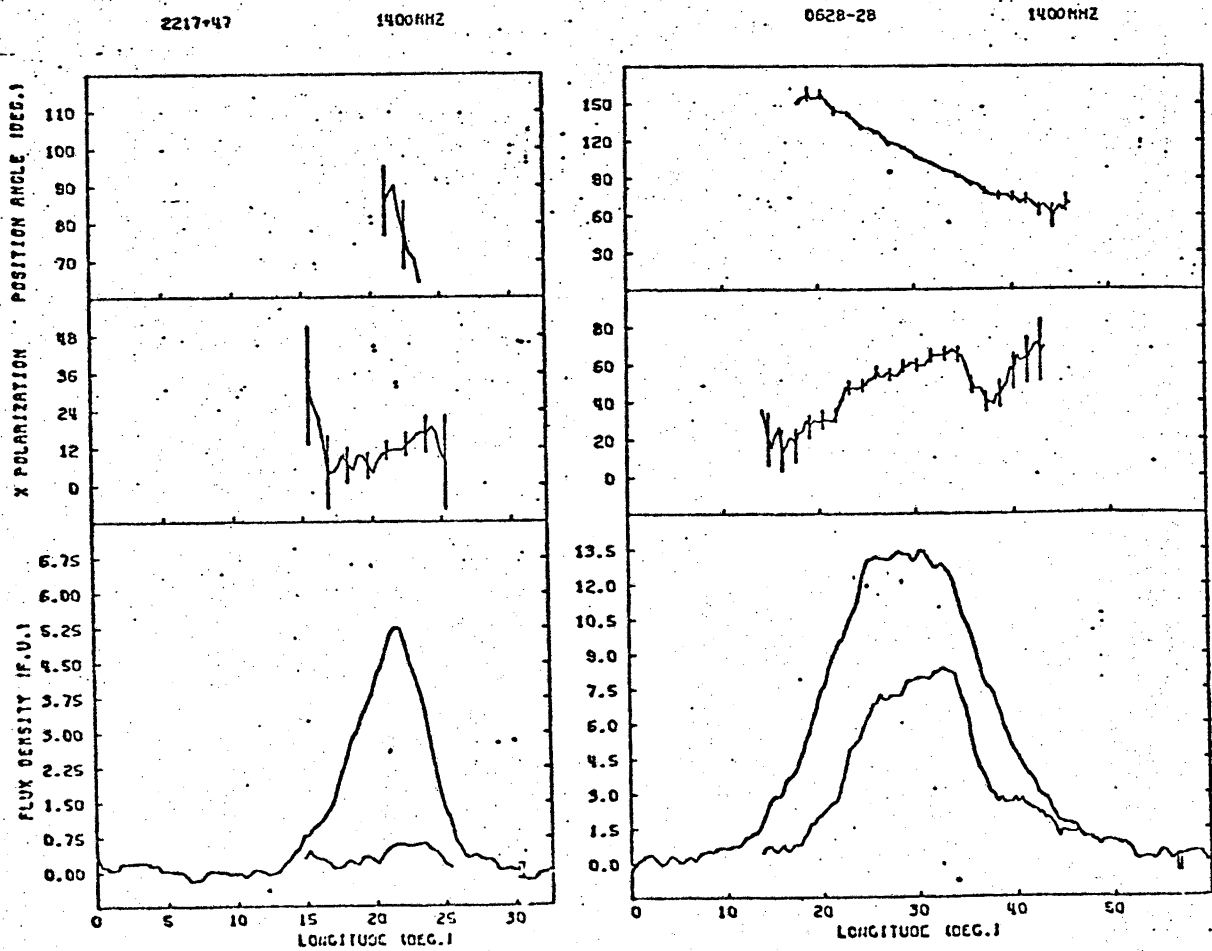
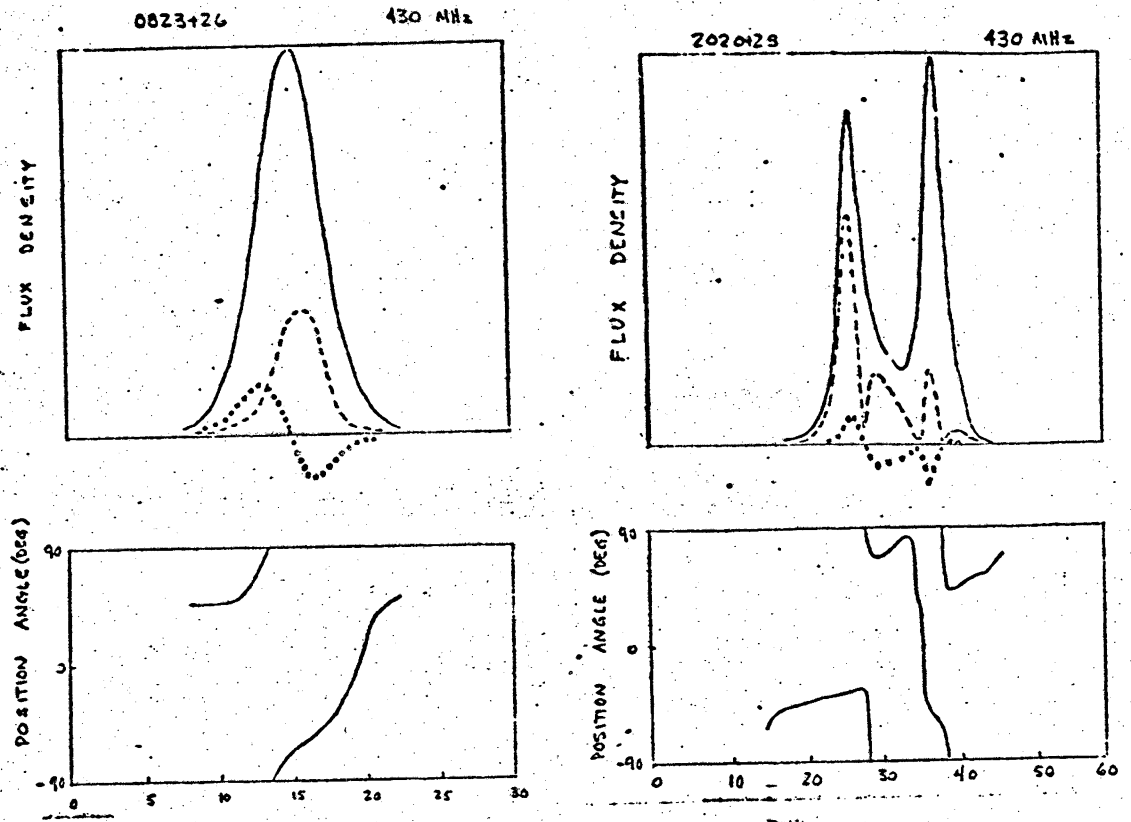


FIG. 9. Polarization profiles. Dashed line above and inner solid line below refer to linear polarization and open dots above refer to circular polarization.

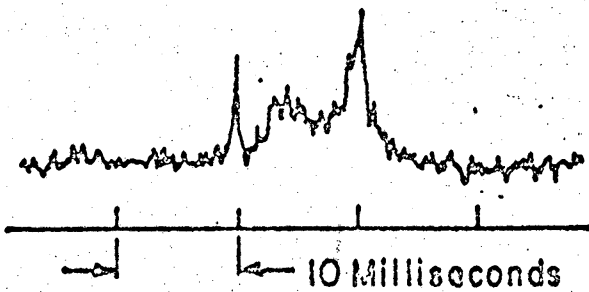
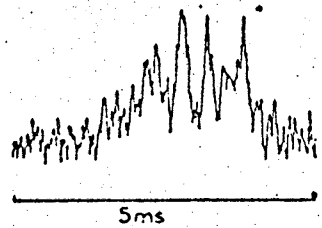
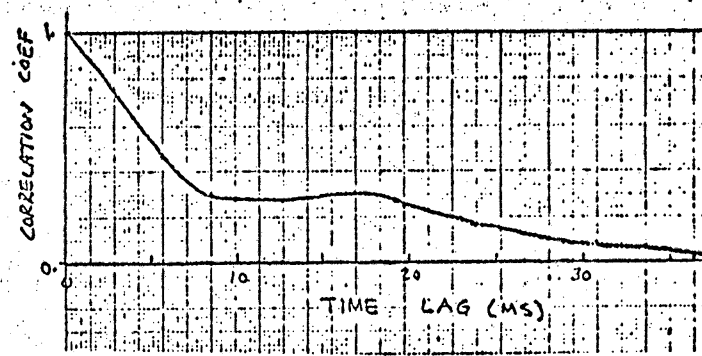
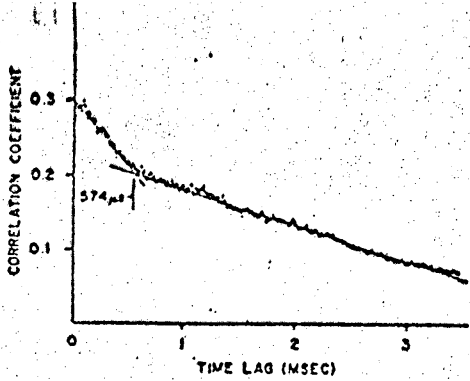


FIG. 10a. Micropulses--at top is an autocorrelation function of 1133+16 data recorded within a small range of a pulse which shows an increase in correlation below 574  $\mu$ s. This behavior indicates the presence of narrow "micropulse" structure. Examples of micropulses are shown at bottom for 0950+08 and 1133+16

FIG. 10b. Subpulses and pulse profile-- at top is an autocorrelation function of 1133+16 data recorded across the entire pulse window defined by the average profile. The decreasing correlation from 0 to 7 ms is the same as that in figure a above 574  $\mu$ s and indicates the presence of "subpulse" structure. The remaining correlation above 7 ms indicates that more than one subpulse occurs in a given pulse window as shown below. The average profile will obviously be double peaked in 1133+16.

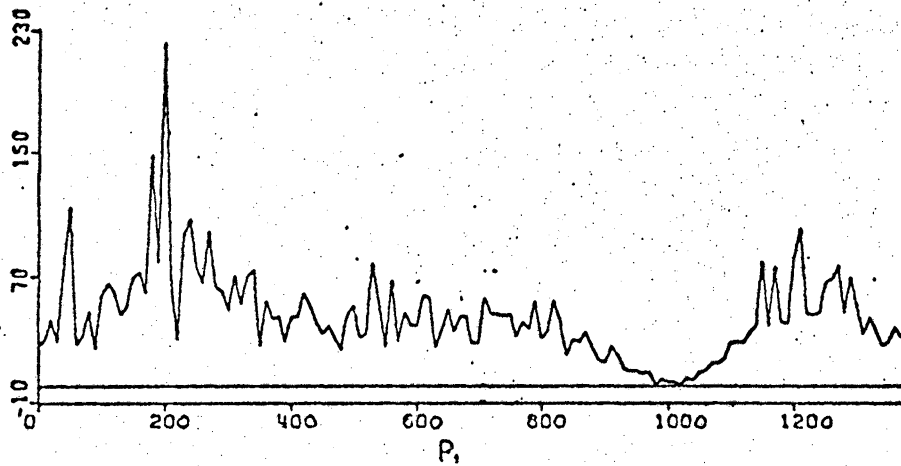
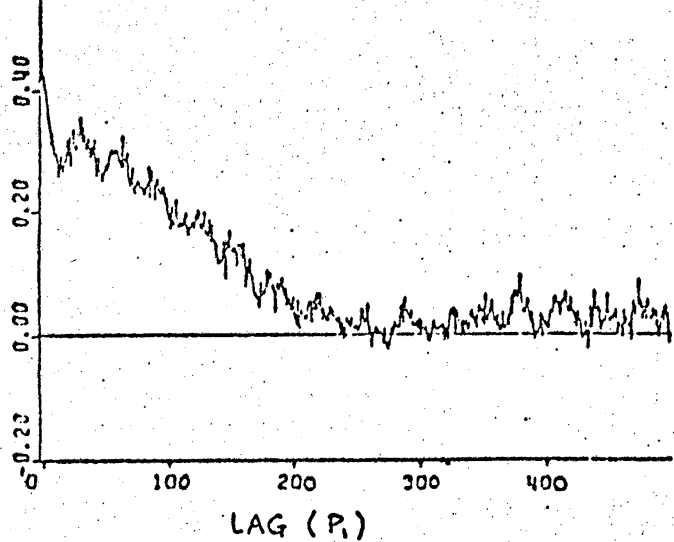


FIG. 10c. Pulse-to-pulse correlations and interstellar scintillation--at top is an autocorrelation function of the pulse energy data of 1133+16 displayed below. 1400 periods is about 30 minutes. The data has been smoothed by a running mean over 10 periods. In the autocorrelation function one sees correlation for a few periods near zero lag, a 50-period oscillation out to 100-200 periods and a broad correlation from scintillation which goes to zero at about 250 periods.

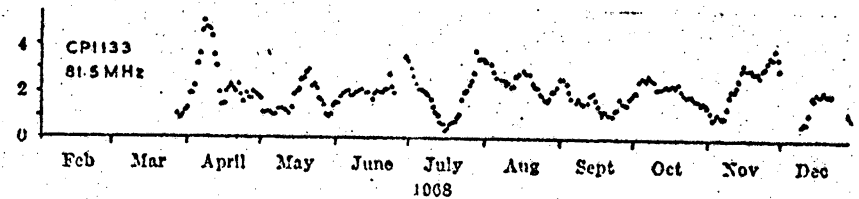
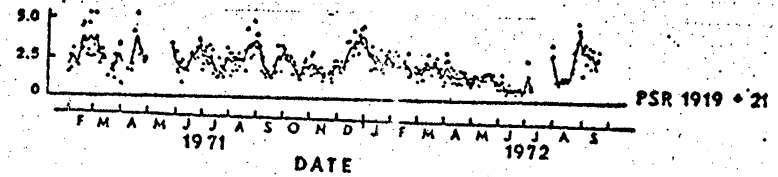
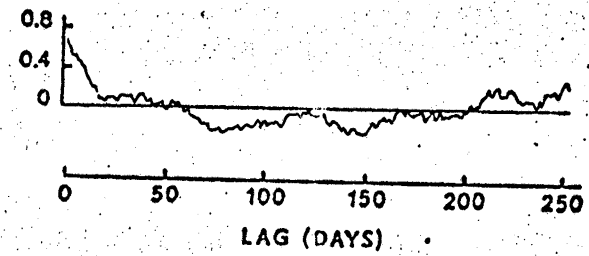


FIG. 10d. Long-term flux variations--at top is a smoothed autocorrelation function of the 1919+21 daily flux data displayed below showing a correlation for about 5-10 days. At bottom are repeated flux measurements of 1133+16.

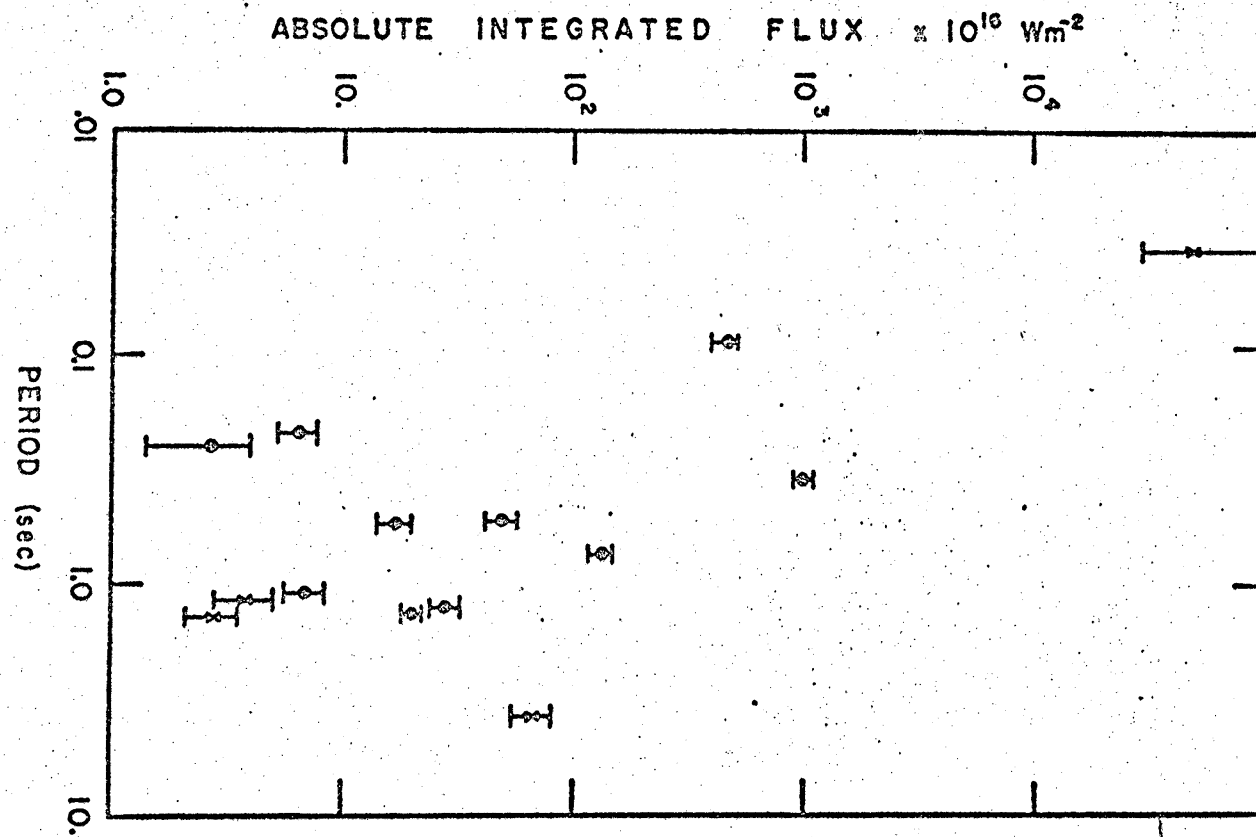


FIG. 11. Correlation of pulsar luminosity and period.

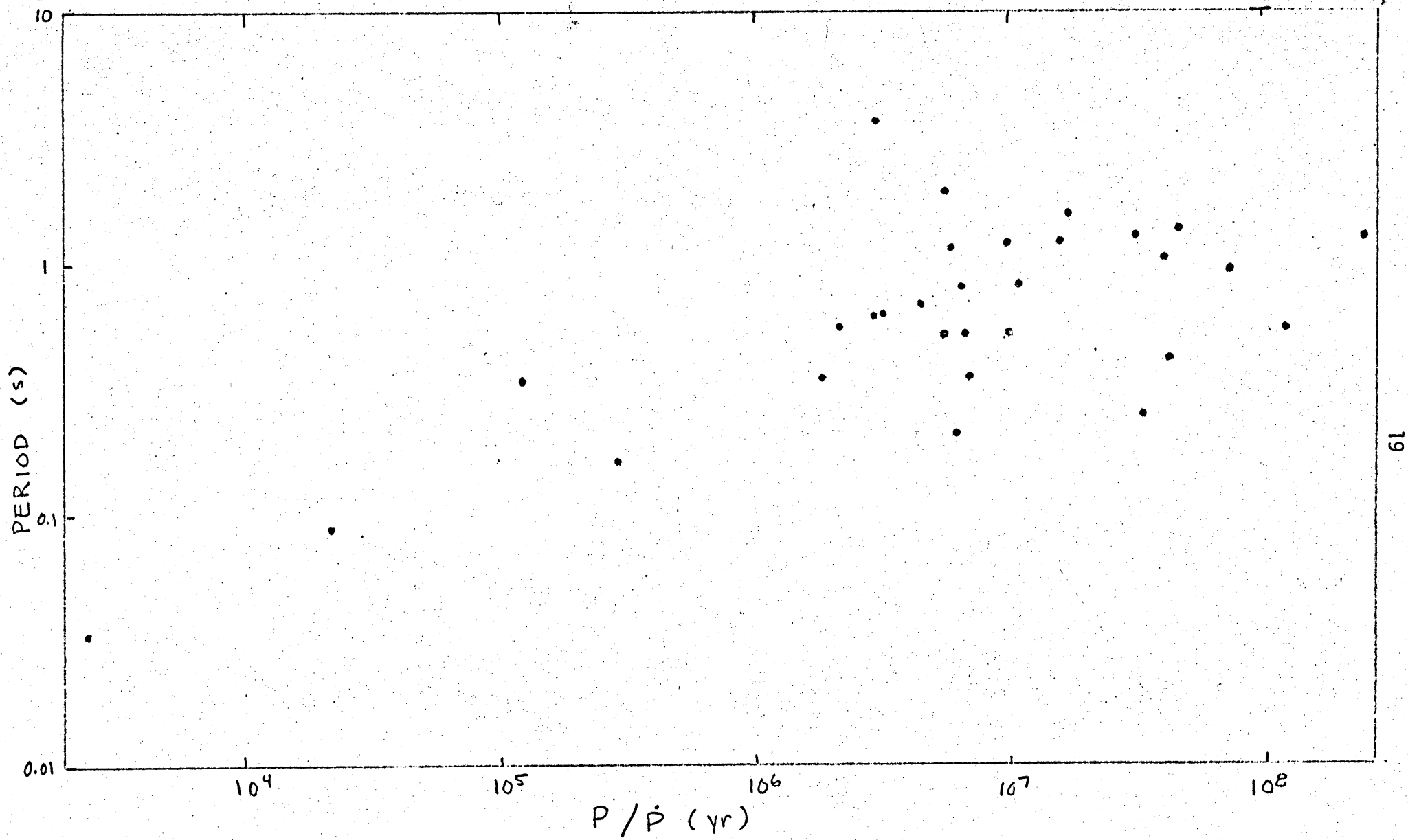


FIG. 12. Correlation of pulsar period and spin-down time,  $P/\dot{P}$ .

A FEW REFERENCESA. REVIEW

- M. Ruderman 1971, Scientific American, 224, No. 2.  
 J. Ostriker 1971, Scientific American, 224, No. 1  
 A. Hewish 1970, Ann. Rev. Ay. Ap., 8, p. 265.  
 Tilson 1970, IEEE Spectrum, Feb. 1970, p. 40.  
 IAU Symposium No. 46 Proceedings, 1970, Jodrell Bank.  
 D. Ter Harr 1972, Physics Reports, 3C, p. 57.  
 H. Y. Chin, PASP.

B. DISCOVERY

- Pulsating Stars, two volumes of reprints from Nature.

C. PROPAGATION EFFECTS

- Dispersion and Rotation measures: R. N. Manchester, 1972, Ap. J., 172, 43.  
 Scintillation: B. J. Rickett 1970, M.N.R.A.S., 150, 67.  
 K. R. Lang 1971, Ap. J., 164, 249.  
 J. Galt and A. G. Lyne 1972, M.N.R.A.S., 158, 281.

D. INTRINSIC PHENOMENA

- Spectra: Hewish above; D. C. Backer 1972, Ap. J. (Letters), 174, L157.  
 \_\_\_\_\_ 1973, submitted to Ap. J. (in library).  
 Polarization: R. N. Manchester 1971, Ap. J. Suppl. Ser., 23, 283.  
 Subpulse phenomena: J. H. Taylor, G. R. Huguenin 1971, Ap. J., 167, 273.  
 A. G. Lyne, F. G. Smith, D. A. Graham 1971,  
M.N.R.A.S., 153, 337.  
 D. C. Backer 1973, Ap. J., 185, 245.  
 Micropulse phenomena: T. H. Hankins 1972, Ap. J. (Letters), 172, L11.

E. THEORY

- P. Goldreich and W. H. Julian 1969, Ap. J., 157, 869.  
 P. A. Sturrock 1971, Ap. J., 164, 529.  
 F. G. Smith 1970, M.N.R.A.S., 149, 1.  
 M. M. Kommisaroff 1970, Nature, 225, 612.